



Experimental Study on Ultimate Strength of Steel Tube Column Filled with Reactive Powder Concrete

Bahaa Al-Abbas¹, Zainab M.R. Abdul Rasoul¹ , Dhafer Hasan¹, Sajjad E. Rasheed^{1*}

¹ Department of Civil Engineering, College of Engineering, University of Kerbala, Kerbala, Iraq.

Received 23 January 2023; Revised 14 May 2023; Accepted 22 May 2023; Published 01 June 2023

Abstract

Composite concrete Filled Tubular Steel (CFT) members, which have excellent deformability due to the well-known confined and constrained interaction between steel tube and concrete, have largely been utilized as bridge piers or columns in high-rise buildings, resulting in increased strength and decreased column size. This study examined the experimental performance of steel tube columns filled with reactive powder concrete (RPC) under axial compression. Three sets of columns were used in the experiment, each with variations in shape (square, rectangular, and circular), length-to-diameter ratio, and compressive strength of the RPC. The first set consisted of five columns, while the second and third sets each had seven columns with three different lengths (750 mm, 600 mm, and 450 mm) and two different compressive strengths (54 and 92 MPa). A new numerical model was developed to calculate the ultimate failure load of the columns by considering factors such as the yield strength of steel, the compressive strength of concrete, the column shape, and the ratio of concrete to steel. This model was validated by comparing the results obtained from the experiments to those predicted by the model, as well as by designing equations from various codes. The results showed that the proposed numerical model accurately predicted the ultimate failure load for columns filled with different types of concrete, especially for RPC, while maintaining conservatism compared to the ACI, AISC, and EN codes equations.

Keywords: Steel Column; Hollow Section; Reactive Powder Concrete; Local Buckling; Lateral Displacement.

1. Introduction

Concrete-filled steel tubes (CFST) have grown in popularity in seismic zones in recent years. The composite effect associated with these members, which is caused by the interaction between the steel tube and the concrete core, can improve both the ductility and capacity of the member [1]. Many researchers have studied the behavior of steel tube columns filled with normal concrete, such as Stephen et al. [2], Uenaka et al. [3], Yang & Han [4], Liao et al. [5], and Almamoori et al. [6]. However, it appears that little attention has gone into studying the behavior of a composite member subjected to axial compression with high or ultra-high-strength concrete. Experiments were carried out [7, 8] on concentrically and eccentrically loaded circular, square, and rectangular CFST stub columns filled by high-strength self-compacting concrete with a length-to-diameter (width) ratio of 3. The test findings revealed that there were substantial variations between partially loaded CFST stub columns and the corresponding fully loaded composite columns due to the presence of partially compressive forces. In recent years, structural engineers have been interested in the performance of CFST under axial compression loads with different concrete types. However, design codes for composite columns have not adequately addressed this issue. Moreover, the design formula was proposed by Uenaka et al. [3] based on the

* Corresponding author: sajjad.e@uokerbala.edu.iq

 <http://dx.doi.org/10.28991/CEJ-2023-09-06-04>



© 2023 by the authors. Licensee C.E.J, Tehran, Iran. This article is an open access article distributed under the terms and conditions of the Creative Commons Attribution (CC-BY) license (<http://creativecommons.org/licenses/by/4.0/>).

yield strengths of the tubes and the filled concrete cylinder. In recent years, a novel group of concrete known as reactive powder concrete (RPC) has recently gotten a lot of interest all over the world due to its superior mechanical properties, such as high strength, high ductility, high durability, low shrinkage, and high resistance to corrosion and abrasion. Many researchers have been studying the properties of RPC, such as Hassooni & Al-Zaidee [9] and Muteb & Hasan [10]. The authors showed that the increase in steel fiber improves the compressive and rupture stresses of the developed concrete. Other researchers studied the effect of RPC or UHPC on the behavior of composite sections, such as Luo et al. [11], Hoang et al. [12], and Mi et al. [13]. Based on their results, the strength and hoop coefficient of the developed column increased due to the growth in the ultimate strength of the RPC core, which highlighted an improvement in the ductility of developed columns. Limit studies on the behavior of steel tube columns filled with RPC under axial compression utilizing various cross-sections can be seen in the above preview. As a result, the focus of this work is on utilizing RPC to experimentally and analytically investigate the CFST's performance.

1.1. Research Significance

The purpose of the current study was to experimentally investigate the effect of using RPC on the behavior of CFST under axial compression loads. This is done by changing the column shape, the compressive strength of the concrete, and the length-to-diameter ratio. In addition to the experimental work, a numerical model has been developed to compute the failure load of the developed CFST columns.

2. Experimental Program

2.1. General Description

The behavior of CFST using RPC while exposed to concentric axial compression stress was investigated using nineteen steel columns in this study. High-quality steel with a yield stress of 363 MPa was employed in this research. The details of the test columns are shown in Table 1 and Figure 1.

Table 1. Characteristics and details of the used columns

Group	Column shape	Column symbols	Length (mm)	Section (mm)	Length/Diameter ratio	Thickness (mm)	Compressive strength of concrete (MPa)
1	Square	S10	750	75*75	10	2	-
		S10-54	750		10	2	54
		S8-92	600		8	2	92
		S6-54	450		6	2	54
		S6-92	450		6	2	92
2	Rectangular	R10	750	75*100	10	2	-
		R10-54	750		10	2	54
		R10-92	750		10	2	92
		R8-54	600		8	2	54
		R8-92	600		8	2	92
		R6-54	450		6	2	54
		R6-92	450		6	2	92
3	Circular	C10	750	75 Dia.	10	2	-
		C10-54	750		10	2	54
		C10-92	750		10	2	92
		C8-54	600		8	2	54
		C8-92	600		8	2	92
		C6-54	450		6	2	54
		C6-92	450		6	2	92

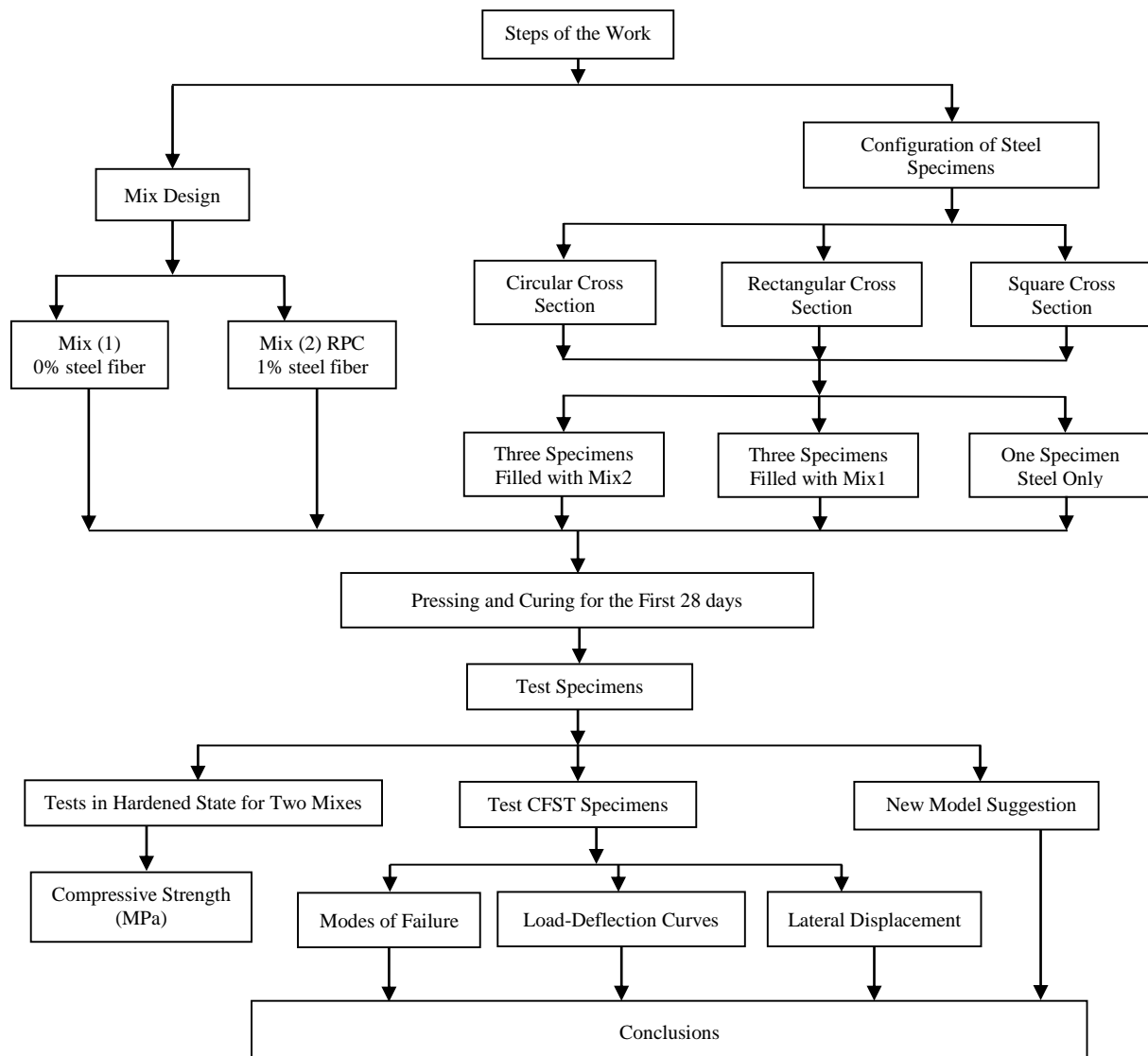


Figure 1. Flowchart for Process of Work

2.2. Materials

A CRESTA 42.5R cement was used in this study. This type of Portland Limestone cement agrees to ASTM C150/C150M–22 [14]. Locally available fine sand with a maximum particle size of 600µm (0.6mm) was used to produce the RPC. Fine aggregate testing was carried out in accordance with [15]. Master Glenium 51's commercial brands of additive (superplasticizer) were used. It's a non-hazardous third-generation superplasticizer produced by BASF–The Chemical Company. The steel fibers used in this study were straight steel wire, which has an aspect ratio (length to diameter) of about 59. ConMix Company's microsilica fume was employed as a mineral additive in the combination. Based on earlier research done by Muteb and Hasan [10], the mixes were employed to achieve maximum compressive strength after trial mixes. The details of the mixes are shown in Table 2. Following that, all specimens were cast and cured inside curing tanks at 60 C° for twenty-eight days.

Table 2. Concrete mixture proportions

Mix	Cement kg/(m) ³	Sand kg/(m) ³	S.F* kg/(m) ³	w/C**	super plasticizer, L/m ³	Steel Fiber %	Steel Fiber kg/m ³
M54***	900	1050	100	0.20	45	0%	0
M92****	900	1050	100	0.20	45	1.5%	117.75

*S.F: silica fume, **W/C: water to cementitious (cement + silica fume) ratio, ***M54: mix with compressive strength 54 MPa, ****M92: mix with compressive strength 92 MPa.

2.3. Instruments and Procedure

After 28 days, all of the columns were removed from the curing water tank, dried, cleaned, and painted. Typical testing equipment with a 2000 kN capacity was used to provide axial compression force on the columns supported by a

stiff, thick plate (20 mm). The plate is used to transfer the axial load from the machine to the column. Three Linear Variation Displacement Transducers (LVDT) sensors with a 0.001 precision were used. The first one records the axial deformation, while the second measures the lateral deformation of the developed CSFT columns, as shown in Figure 2. When each tested column's resistance decreased (the loading curve levelled), the loading was terminated.

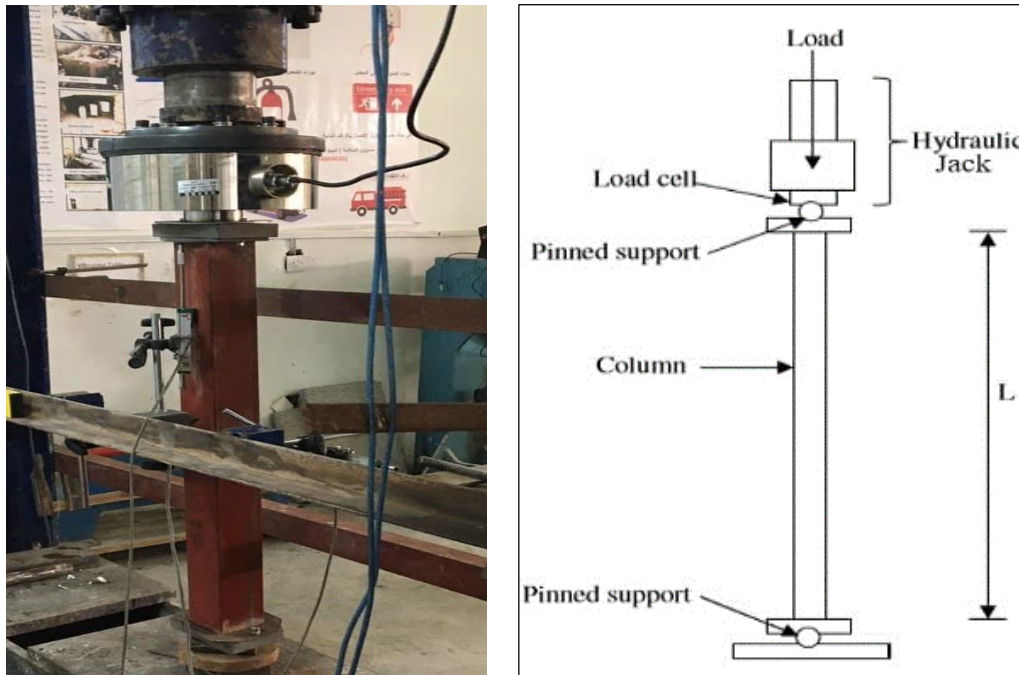


Figure 2. CFST Column Testing Equipment

3. Experimental Results and Discussion

3.1. Modes of Failure

Figure 3 illustrates the failure modes of the tested CFST columns. At first, all columns were in the elastic stage, then moved to the elastic-plastic phase. Local yielding began to appear at the ends of each column as the axial load increased due to stress concentration. All columns collapsed with local buckling at the ends during the last phases of loading; these results were comparable to those found by Luo et al. [11]. In general, the RPC that filled steel tube columns increased the compressive strength, delaying the failure of all columns. Also, the circular shape is more resistant to failure compared to square and rectangular ones. The results also showed that the length-to-diameter ratio was less effective compared to other variables.



Figure 3. Failure Modes for Tested CFST Columns

3.2. Load-Deflection Curves

With various weights, the vertical displacement of the tested columns was recorded and drawn. The effects of three factors on load-deflection behavior were investigated as follows:

3.3. Length to Diameter Ratio Effect

The effects of the length-to-diameter ratio on the behavior of load-vertical displacement are shown in Figure 4 and Table 3. It can be seen that there is a significant improvement in the behavior of all filled columns compared with reference columns (without filling using RPC). The column filled with RPC (compressive strength of 92 MPa) is stiffer in behavior compared to a column filled with concrete (compressive strength of 54 MPa). This is due to the stiffer behavior of RPC containing microsteel fiber. And it can be observed that the presence of steel fiber makes the behavior of the curve stiffer for shorter columns and the stage after ultimate load more ductile for intermediate circular columns, which corresponds with the results of Hoang et al. [12]. The failure load for all shapes increased as the compressive strength of concrete increased. However, the failure load for the square and rectangular columns is less than the failure load for the circular columns when using the same concrete.

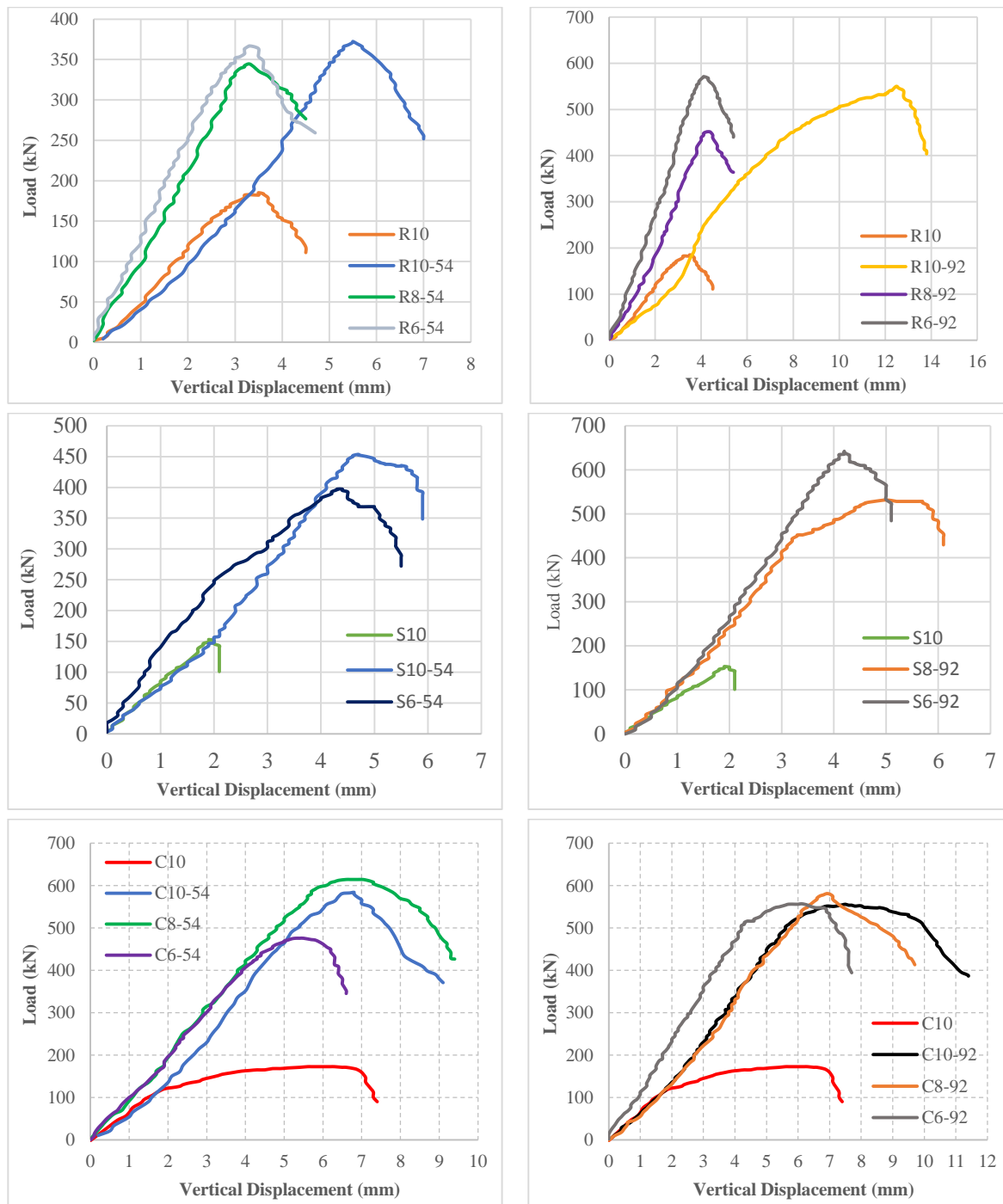


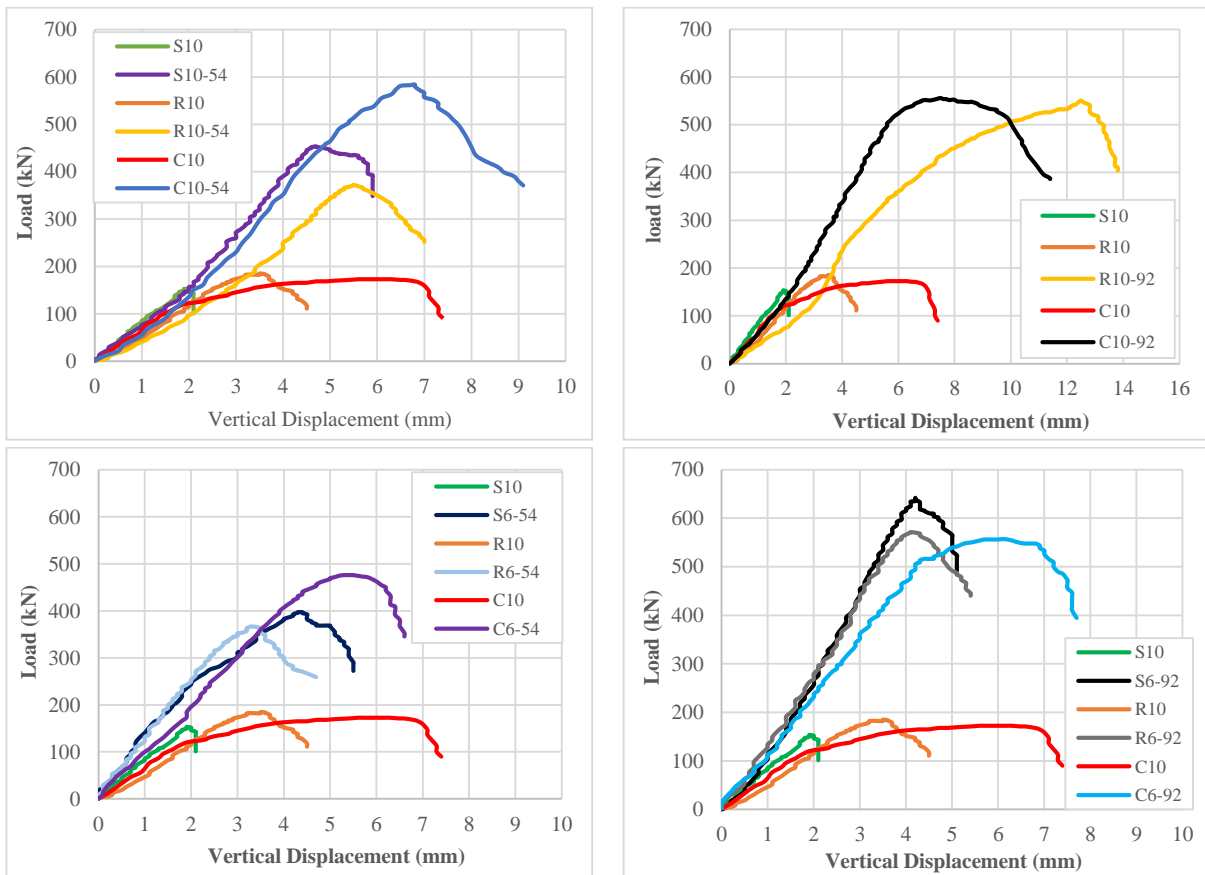
Figure 4. Effect of Length to Diameter Ratio Columns

Table 3. The Tests Results of Columns

Group	Column shape	Column symbols	Failure Load (kN)	Vertical displacement (mm)	Lateral displacement (mm)	
					X-direction	Y-direction
1	Square	S10	153.2	2.022	1.16	0.5
		S10-54	452.7	5.573	0.76	0.49
		S8-92	531.3	5.801	-0.17	0.79
		S6-54	392.8	5.042	-0.13	1.18
		S6-92	638.8	4.234	-0.5	1.42
2	Rectangular	R10	185.2	4.099	1.79	0.05
		R10-54	372.4	5.860	0.19	-0.17
		R10-92	550.20	13.295	1.9	0.6
		R8-54	344.6	4.158	-0.73	0.53
		R8-92	451.9	5.018	-0.01	-0.003
		R6-54	366.9	4.724	0.88	0.81
		R6-92	571.4	4.203	-0.09	0.68
3	Circular	C10	172.7	6.389	-0.146	Not available
		C10-54	584.3	7.12	-0.52	1.19
		C10-92	556	10.252	-0.005	1.28
		C8-54	614.5	7.115	-0.27	0.32
		C8-92	581.1	8.293	-1.6	0.92
		C6-54	475.8	5.947	-0.75	1.36
		C6-92	557.1	6.886	-0.71	0.87

3.4. Compressive Strength Effect

The influence of compressive strength on vertical displacement behavior is seen in Figure 5. It can be noticed that the compressive strength has a significant effect on the behavior of each column. The columns filled with 92 MPa compressive strength concrete performed better than the columns filled with 54 MPa concrete by 62.5%, 54%, and 16.5% for the square, rectangular, and circular columns, respectively. From that, it can be concluded that the columns with higher compressive strength exhibit stiffer behavior; these results correspond to those found by Hoang et al. [12].



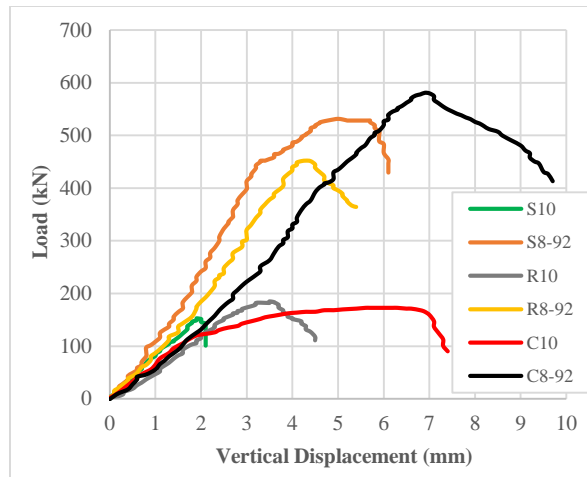


Figure 5. Effect of compressive strength on Vertical Displacement

3.5. Lateral Displacement

The relationships between the axial load and lateral displacements at mid-height for all columns are shown in Figures 6 to 8. Small values of lateral displacements in all specimens are noticed and the lateral displacements in the x-direction are smaller than the displacements in the y-direction. This was referred to as the position of local-buckling occurred far from the place of the LVDT, which measured this displacement. In most situations, the columns behaved similarly in terms of lateral displacement in the x and y directions. Besides, the compressive strength of the concrete used as well as the column shape have an insignificant effect on the lateral displacement at mid-height of each column as clearly noticed in Figure 9 for square, rectangular and circular shape.

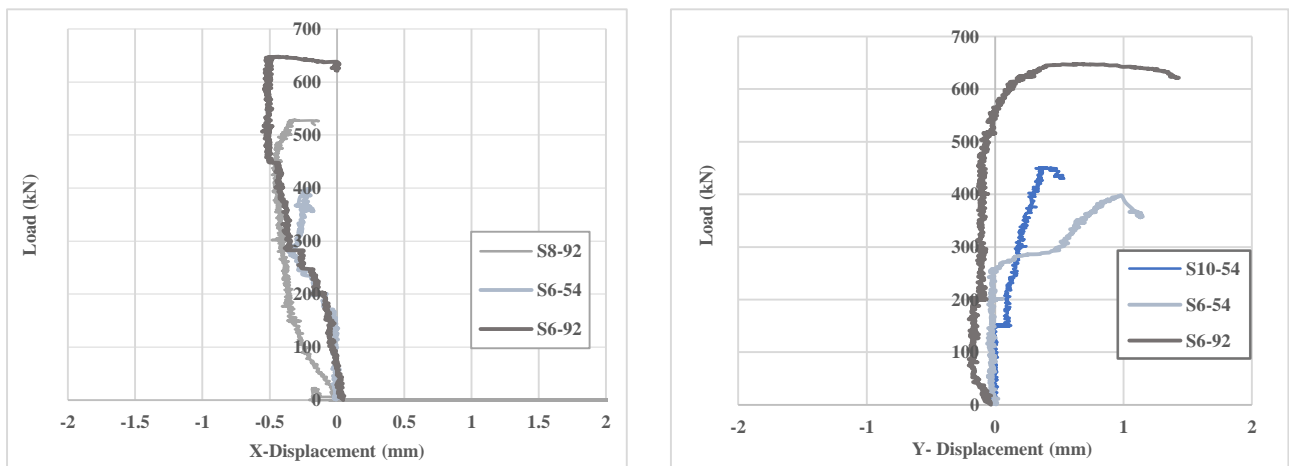


Figure 6. Lateral Displacement in Group 1

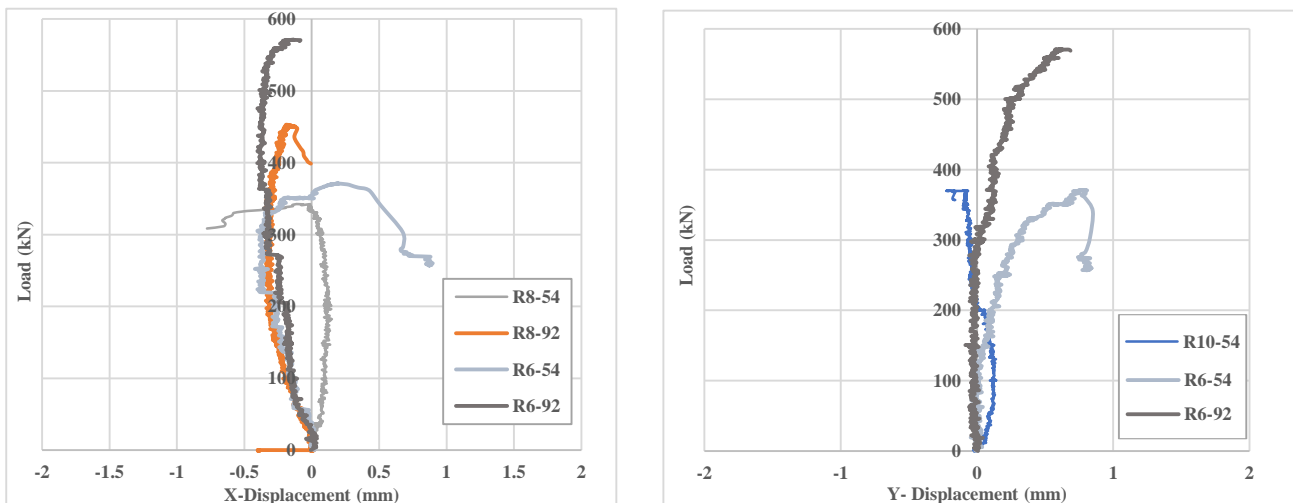


Figure 7. Lateral Displacement in Group 2

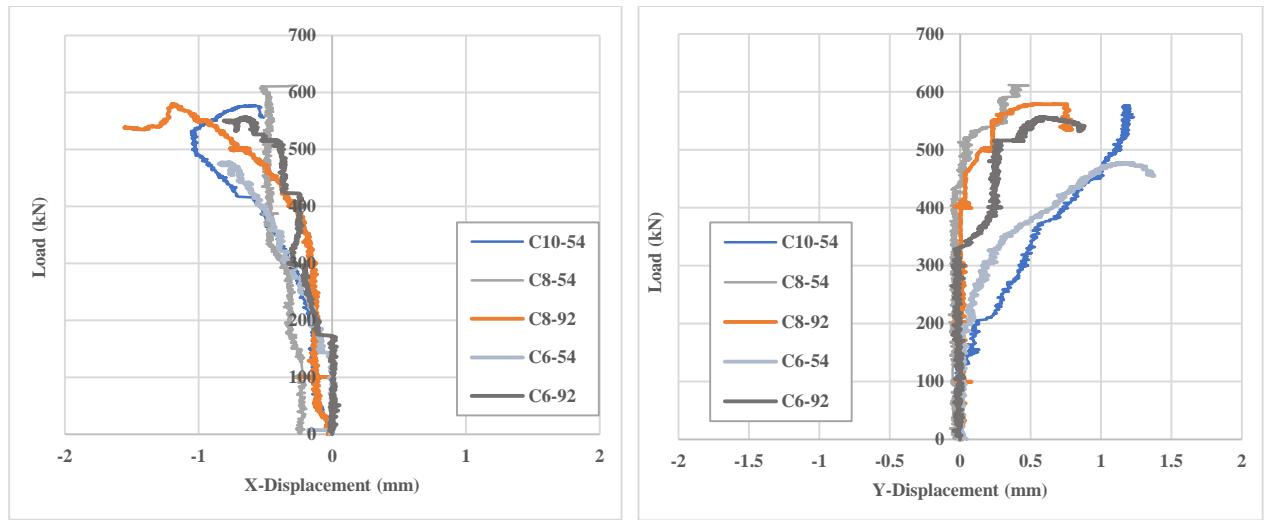


Figure 8. Lateral Displacement in Group 3



Figure 9. Lateral displacement for various sections

3.6. New Model Suggestion

Many equations such as the equations found in ANSI/AISC 360-22 [16], Eurocode 4 [17], and ACI 318 [18] codes are used to determine the strength of concrete-filled columns. Besides, many researchers suggested equations to calculate the compressive strength of concrete-filled columns like [3]. The common questions used to calculate the strength of the circular concrete-filled columns are listed as follows:

$$P_P = A_s f_y + C_2 A_c f'_c \quad (C_2=0.85)(AISC360-16) \tag{1}$$

$$P_{PL,Rd} = A_s f_y + A_c f'_c \quad (EN1994) \tag{2}$$

$$P_U = A_{si} f_{syi} + A_{so} f_{syo} + 0.85 A_c f'_c \tag{3}$$

$$N_{uCFDST} = \left[2.86 - 2.59 \left(\frac{D_i}{D_o} \right) \right] A_{so} f_{syo} + A_{si} f_{syi} + A_c f'_c \quad \left(0.2 < \frac{D_i}{D_o} < 0.7 \right) \quad (\text{Uenaka et al. equation [3]}) \tag{4}$$

The model developed in this research to predict the compressive load of concrete-filled tubular steel column is as follows:

$$Pu = \beta (k_1 A_s f_y + k_2 A_c f'_c) \tag{5}$$

where Pu is the ultimate axial load, β is the shape factor, k_1 and k_2 are variables coefficients.

Regression analysis was done to estimate the impact of each parameter on the performance of the developed model with a coefficient of determination (R^2) equal to 0.982 and the resulted values are:

$$\beta = \left\{ \begin{array}{ll} 0.95 & \text{steel tube} \\ 0.68 & \text{composit rectangular tube} \\ 1.05 & \text{composit square tube} \\ 1.36 & \text{composit circular tube} \end{array} \right\} \tag{6}$$

Table 4 shows the difference between the experimental and theoretical results for all columns. It can be seen that the results of failure load for EN code are higher than the results of AISC and ACI code. Comparing the results of the current research with the results from the aforementioned codes, this study's proposed equation offers a better prediction of the compressive strength than the prediction offered by the codes equations when used to predict the compressive strength for square and circular cross-section. However, this study equation offers a less accurate prediction of the compressive strength for rectangular cross-sections columns compared to different codes equations. It can be concluded from these results that the effect of the cross-section of the column on its performance was clear. The suggested equation, based on R^2 , was able to predict 98% of the change in compressive strength depending on the factors employed.

Table 4. Theoretical and Experimental Axial Compressive Load of All Columns

Column symbols	Experimental axial compressive load (P_u) kN	Theoretical axial compressive load (kN)								
		Compressive strength f'_c MPa	Yield Stress f_y MPa	Area of steel mm^2	Area of concrete mm^2	Steel Fiber Ratio	AISC equation	EN equation	ACI equation	proposed equation
S10	153.2	0	250	584	0	0%	146	146	146	201.39
S10-54	452.7	54	250	584	5041	0%	377.38	418.21	377.38	445.53
S8-92	531.3	92	250	584	5041	1.5%	540.21	609.77	540.21	602.42
S6-54	392.8	54	250	584	5041	0%	377.38	418.21	377.38	445.53
S6-92	638.8	92	250	584	5041	1.5%	540.21	609.77	540.21	602.42
R10	185.2	0	250	684	0	0	171	171	171	235.87
R10-54	372.4	54	250	684	6816	0%	483.85	539.1	483.85	364.059
R10-92	550.20	92	250	684	6816	1.5%	704.01	798.1	704.01	501.43
R8-54	344.6	54	250	684	6816	0%	483.85	539.1	483.85	364.059
R8-92	451.9	92	250	684	6816	1.5%	704.01	798.1	704.01	501.44
R6-54	366.9	54	250	684	6816	0%	483.85	539.1	483.85	364.059
R6-92	571.4	92	250	684	6816	1.5%	704.01	798.1	704.01	501.44
C10	172.7	0	250	458.44	0	0	114.61	114.61	114.61	160.26
C10-54	584.3	54	250	458.44	3957.185	0%	296.24	328.29	296.24	456.103
C10-92	556	92	250	458.44	3957.185	1.5%	424.06	478.67	424.06	615.62
C8-54	614.5	54	250	458.44	3957.185	0%	296.24	328.29	296.24	456.103
C8-92	581.1	92	250	458.44	3957.185	1.5%	424.06	478.67	424.06	615.62
C6-54	475.8	54	250	458.44	3957.185	0%	296.24	328.29	296.24	456.103
C6-92	557.1	92	250	458.44	3957.185	1.5%	424.06	478.67	424.06	615.62

Figure 10-a shows the normal probability plot of the residuals which verifies the assumption of the normal distribution of the residuals. The normal probability plot of the residuals generally follows a straight line. There is no evidence of abnormality, outliers, or unidentified variables. The residuals versus fits plot are used to confirm that the residuals are distributed randomly and have a constant variance. Ideally, the points would fall randomly on both sides of zero, with no discernible patterns. The data appears to be scattered randomly about zero. There is no indication that the residual value is influenced by the fitted values as seen in Figure 10-b. The residuals are not related to one another, as seen in Figure (10-d). When displayed in time order, independent residuals show no trends or patterns. Patterns in the points might suggest that residuals that are near each other are associated and hence are not independent. The residuals should appear to fall randomly around the centreline.

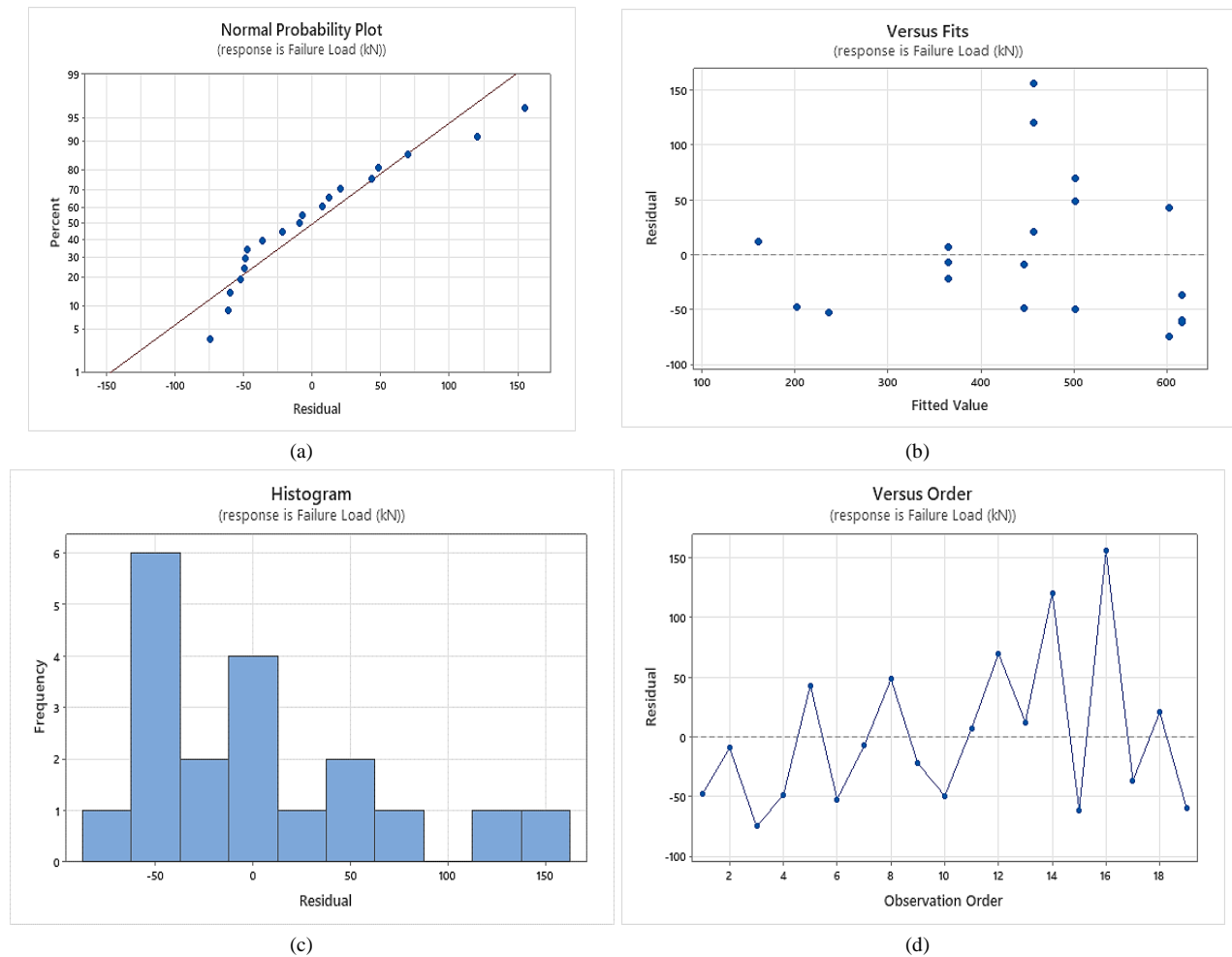


Figure 10. The Results of Statistical Analysis

4. Conclusion

This study has investigated the performance of steel tube columns filled with reactive powder concrete (RPC) under axial compression with different cross sections. The collected test data from nineteen specimens was analyzed and compared with previous studies and design codes. The following conclusions can be drawn from the present study.

Due to the high compressive strength and presence of steel fiber, the composite effect caused by the interaction between the steel tube and the concrete core can improve both the ductility and capacity of the member. On the other hand, the failure mode of the columns filled with RPC differs from that of the columns filled with normal concrete. As a result, local buckling and local yielding appeared at the ends of the column due to some stress concentration at these locations. The behavior of the columns in terms of load-vertical displacement is stiffer with the increase in compressive strength due to the use of RPC with micro-steel fiber. The maximum ratios of increase in displacement resistance with increase in compressive strength were 62.5%, 54%, and 16.5% for square, rectangular, and circular columns, respectively. Also, with respect to the effect of shape, circular columns have a better vertical displacement compared with other shapes, as the displacement resistance increased by 28.5% and 20% for rectangular and square columns, respectively. While the lateral displacement was unaffected by the compressive strength or shape of the columns, this is attributed to the confinement effect. In addition to these main findings in the part of experimental results, there are some concluded remarks about the theoretically proposed equation, which, despite its limitations to pinned boundary

conditions and concentrated axial load. Furthermore, it provided an accurate prediction while remaining conservative compared with the underestimated results offered by the ACI, AISC, and EN codes equations. In details, the enhancement of concrete capacity within the section represented by the parameter k_2 converges the results of the proposed equation with the values obtained from the experimental test, and the shape factor β is very sensitive and affects the ultimate capacity of the CFST column.

5. Nomenclature

RPC	Reactive Powder Concrete	LVDT	Linear Variation Displacement Transducers
CFST	Concrete-filled steel tubes	Pu	Ultimate axial load
β	Shape Factor	k_1, k_2	Variable coefficients
FE	Finite Element	ACI	American Concrete Institute
OPC	Ordinary Portland cement	AISC	American Institute of Steel Construction
UHPC	Ultra-High-Performance Concrete	EN	European Standard

6. Declarations

6.1. Author Contributions

Conceptualization, B.A. and D.H.; methodology, B.A. and D.H.; software, B.A. and S.E.R.; validation, B.A. and Z.M.R.A.; formal analysis, B.A. and Z.M.R.A.; investigation, B.A. and D.H.; resources, B.A. and Z.M.R.A.; data curation, B.A. and D.H.; writing—original draft preparation, B.A. and Z.M.R.A.; writing—review and editing, B.A. and S.E.R.; visualization, B.A. and S.E.R.; supervision, B.A. and D.H.; project administration, B.A.; funding acquisition, B.A. and D.H. All authors have read and agreed to the published version of the manuscript.

6.2. Data Availability Statement

The data presented in this study are available in the article.

6.3. Funding

The authors received no financial support for the research, authorship, and/or publication of this article.

6.4. Conflicts of Interest

The authors declare no conflict of interest.

7. References

- [1] Jiang, Y., Silva, A., Macedo, L., Castro, J. M., Monteiro, R., & Chan, T. M. (2019). Concentrated-plasticity modelling of circular concrete-filled steel tubular members under flexure. *Structures*, 21, 156–166. doi:10.1016/j.istruc.2019.01.023.
- [2] Schneider, S. P., Kramer, D. R., & Sarkkinen, D. L. (2004). The design and construction of concrete-filled steel tube column frames. 13th World Conference on Earthquake Engineering, 1-6 August, 2004, Vancouver, Canada.
- [3] Uenaka, K., Kitoh, H., & Sonoda, K. (2010). Concrete filled double skin circular stub columns under compression. *Thin-Walled Structures*, 48(1), 19–24. doi:10.1016/j.tws.2009.08.001.
- [4] Yang, Y. F., & Han, L. H. (2012). Concrete filled steel tube (CFST) columns subjected to concentrically partial compression. *Thin-Walled Structures*, 50(1), 147–156. doi:10.1016/j.tws.2011.09.007.
- [5] Liao, F. Y., Hou, C., Zhang, W. J., & Ren, J. (2019). Experimental investigation on sea sand concrete-filled stainless steel tubular stub columns. *Journal of Constructional Steel Research*, 155, 46–61. doi:10.1016/j.jcsr.2018.12.009.
- [6] Almamoori, A. H. N., Naser, F. H., & Dhahir, M. K. (2020). Effect of section shape on the behaviour of thin walled steel columns filled with light weight aggregate concrete: Experimental investigation. *Case Studies in Construction Materials*, 13. doi:10.1016/j.cscm.2020.e00356.
- [7] Han, L. H., Liu, W., & Yang, Y. F. (2008). Behaviour of concrete-filled steel tubular stub columns subjected to axially local compression. *Journal of Constructional Steel Research*, 64(4), 377–387. doi:10.1016/j.jcsr.2007.10.002.
- [8] Yang, Y. F., & Han, L. H. (2011). Behaviour of concrete filled steel tubular (CFST) stub columns under eccentric partial compression. *Thin-Walled Structures*, 49(2), 379–395. doi:10.1016/j.tws.2010.09.024.
- [9] Hassooni, A. N., & Al-Zaidee, S. R. (2022). Rehabilitation of Composite Column Subjected to Axial Load. *Civil Engineering Journal*, 8(3), 595-611. doi:10.28991/CEJ-2022-08-03-013.

- [10] Muteb, H. H., & Hasan, D. M. (2020). Ultra-high-performance concrete using local materials and production methods. IOP Conference Series: Materials Science and Engineering, 870, 012100. doi:10.1088/1757-899X/870/1/012100.
- [11] Luo, H., Wang, W., Shen, L., & Wang, G. (2017). Stress-strain model for reactive powder concrete confined by steel tube. Journal of Engineering Science and Technology Review, 10(2), 122–131. doi:10.25103/jestr.102.15.
- [12] Hoang, A. Le, Fehling, E., Lai, B., Thai, D. K., & Chau, N. Van. (2019). Experimental study on structural performance of UHPC and UHPFRC columns confined with steel tube. Engineering Structures, 187, 457–477. doi:10.1016/j.engstruct.2019.02.063.
- [13] Mi, Y., Liu, Z., Wang, W., Yang, Y., & Wu, C. (2020). Experimental study on residual axial bearing capacity of UHPFRC-filled steel tubes after lateral impact loading. Structures, 26, 549–561. doi:10.1016/j.istruc.2020.04.032.
- [14] ASTM C150/C150M-22. (2022). Standard Specification for Portland Cement. ASTM International, Pennsylvania, United States. doi:10.1520/C0150_C0150M-22.
- [15] Iraqi Specifications No.45. (1984). Aggregates of Natural Resources used for Concrete and Construction. Iraqi Specifications, Baghdad, Iraq.
- [16] ANSI/AISC 360-22. (2022). Specification for Structural Steel Buildings. American Institute of Steel Construction, Illinois, United States.
- [17] Eurocode 4. (2014). Design of composite steel and concrete structures. European Committee for Standardization, Brussels, Belgium. doi:10.1007/978-3-642-41714-6_51757.
- [18] ACI 318. (1994). Building Code Requirements for Structural Concrete and Commentary. American Concrete Institute (ACI), Michigan, United States.